Innovative Food Science and Emerging Technologies 41 (2017) 292–300

Contents lists available at ScienceDirect

Innovative Food Science and Emerging Technologies

journal homepage: www.elsevier.com/locate/ifset

Experimental comparison of microwave and radio frequency tempering of frozen block of shrimp

T. Koray Palazoğlu*, Welat Miran

Department of Food Engineering, Mersin University, 33343 Mersin, Turkey

ARTICLE INFO

Keywords:
Tempering
Microwave
Radio frequency
Frozen shrimp

ABSTRACT

In this study, microwave and radio frequency tempering of frozen shrimp were compared experimentally in terms of tempering rate and uniformity. To do this, a block of frozen shrimp (1.75 kg) was tempered from an initial temperature of − 22 °C to between − 5 and − 3 °C both in a microwave system (915 MHz) and a radio frequency oven (27.12 MHz). Temperatures at four different internal locations were recorded during tempering experiments by using a signal conditioner and fiber optic probes. Surface temperature was also measured using an infrared camera immediately after tempering. Time needed for temperature increase from the initial to between − 5 and − 3 °C at all four locations where the fiber optics were inserted was about 10 and 4 min for power settings of 500 W and 1 kW respectively when microwave tempering was performed. In case of radio frequency tempering, it took 11 and 7 min to reach between − 5 and − 3 °C at all four locations for electrode gaps of 160 and 150 mm, respectively. Among all treatments, microwave tempering at 500 W yielded the most uniform internal temperature distribution. However, local surface overheating was observed during microwave tempering at both power settings. Radio frequency tempering, in contrast, was found to result in a uniform overall temperature distribution with no local overheating at the surface.

1. Introduction

Frozen foods are usually thawed or tempered before further processing in food industry. In thawing, thermal center of the frozen product reaches 0 °C. However, lower temperatures (usually − 5 to − 2 °C) are targeted in tempering. At this temperature range the frozen product is not completely thawed but softened, and hence can readily be further processed (Yarmand and Homayouni, 2011).

Thawing of frozen blocks of meat and seafood by microwave and radio frequency has been commercially applied due to several advantages of electromagnetic thawing over conventional thawing methods. These advantages include reduced thawing time and less damage to product quality owing to the volumetric heating characteristic of electromagnetic energy. In addition, drip loss is minimized and microbial safety is not compromised when electromagnetic thawing methods are used (Li and Sun, 2002).

Comparison of electromagnetic and conventional thawing in terms of tempering rate and uniformity has been conducted in several studies (Farag et al., 2008a and 2011; Zhao et al., 2000). Farag et al. (2008a and 2011) showed that radio frequency application provides significant reduction in tempering time (from hours and even days to minutes) when compared to conventional air tempering. An 85-fold reduction in tempering time along with a comparable uniformity of temperature distribution was reported by Farag et al. (2011) when RF tempering was employed. Farag et al. (2008a) compared the temperature distributions in 4-kg beef blends tempered by radio frequency (27.12 MHz) and conventional air tempering. In RF tempering experiments, they targeted temperatures between − 5 and − 2 °C and reported that 11 min at 500 W was the optimum RF power-time combination yielding an average temperature of − 3.6 ± 1.1 °C. They found in another study (Farag et al., 2011) however that when higher temperatures (− 1 to 5 °C) were targeted (thawing), a considerably longer time (35 min) was needed at 400 W as completion of the phase change zone required a large amount of energy (Fu, 2004). Wang and Goldblith (1976) also showed that twice as much energy was required to temper frozen beef from − 17.7 °C to − 2.2 °C than to temper it to − 4.4 °C. Furthermore, the optimum treatment in terms of temperature distribution was obtained by employing a power program (20 min on + 10 min off + 15 min on). Again, Zhao et al. (2000) reported 12.5 min for RF thawing, 3 h for water and 16 h for air thawing for 3.18 kg block of kippers (38.1 × 25.4 × 3.8 cm).

Comparative study of radio frequency and microwave heating was performed only by a limited number of researchers (Dubey et al., 2016; Choi et al., 2017). Dubey et al. (2016) used a 19 MHz RF system and a

* Corresponding author.
E-mail address: koray_palazoglu@mersin.edu.tr (T. Koray Palazoğlu).

http://dx.doi.org/10.1016/j.ifset.2017.04.005
Received 16 January 2017; Received in revised form 7 April 2017; Accepted 11 April 2017
Available online 12 April 2017

2.45 GHz microwave oven with an equivalent heating power (3.4 kW) and measured temperature at different depths of wood. While similar heating rates were observed for RF and microwave treating of wood with cross-sectional dimensions of 10 × 10 to 15 × 15 cm, > 40% faster and more uniform heating was achieved with the RF system when the dimension was above 15 × 15 cm. Choi et al. (2017) investigated the effect of various tempering methods (forced air, water immersion, radio frequency, and microwave) on tempering rate of frozen pork loin (100 × 100 × 70 mm). A 19-fold reduction in tempering time (time to bring pork loin from −20 to −2 °C) was observed with the radio frequency system when compared to forced air treatment. Microwave tempering was, however, found to be the fastest method of all. It should be noted here that a domestic microwave oven operating at 2.45 GHz was used in their study.

In the present study, tempering performances of a microwave and a radio frequency system operating at frequencies commonly used in industrial scale thawing equipment were experimentally compared in terms of tempering rate and uniformity. Tempering at two different power settings in both methods were studied by using a frozen block of shrimp as the model.

2. Materials and methods

Tiger shrimps (75–80 count per kg, moisture content 81% by weight), peeled/beheaded and weighing 1.75 kg, were frozen as a block (23.0 × 16.8 × 5.0 cm) in a cardboard box using a top-loading freezer (Arçelik, Model 2536 A + + D, Turkey) with a capacity of 232 L.

2.1. Microwave tempering

Microwave tempering system (Sonar, Izmir, Turkiye) specially designed in our laboratory consisted of a 5 kW magnetron operating at 915 MHz, a rectangular waveguide and a cylindrical cavity (Fig. 1). System power was adjustable in 500 W intervals. The cavity (25.4 cm height and 54.0 cm diameter) had a removable top cover with a 25-mm hole in the center. This hole was used to run the fiber optic temperature probes into the cavity. The system was equipped with a turntable to improve heating uniformity. In fact, rotation was required during microwave treatment in order to avoid runaway heating. The turntable completed one revolution in 88 s. The frozen block in cardboard box with its top open was placed on the turntable in the center of the cavity. The orientation of the block with respect to the waveguide was the same in all experiments when the system was turned on. Microwave tempering experiments at two different power settings (500 W and 1 kW) were conducted in duplicate.

2.2. Radio frequency tempering

Radio frequency tempering was conducted by using a laboratory scale free-running oscillator radio frequency (RF) system with a parallel plate electrode design operating at a frequency of 27.12 MHz and a maximum power of 2 kW (Sonar, Izmir, Turkiye) (Fig. 2). Electrode width and length were 43 cm and 100 cm, respectively. The top electrode was movable so that the gap between the electrodes could be adjusted. The largest gap setting that can be adjusted in the RF system was 160 mm, while 150 mm was the lowest gap setting that can be used in order to avoid bending of the fiber optic probes. Radio frequency tempering experiments were conducted in duplicate at electrode gap settings of 150 and 160 mm. The frozen block of shrimp in cardboard box was placed on a turntable between and in the horizontal center of the electrodes. Radio frequency tempering was employed with and without rotation (horizontal) to see the possible effect of moving the sample on heating uniformity. The distance between the upper surface of the block and the top electrode was 46 and 56 mm for the gap settings of 150 and 160 mm, respectively.

2.3. Temperature measurement

Temperatures at four different internal locations were recorded with 1 sec interval by using a 4-channel signal conditioner and fiber optic probes (UMI-4, FISO, Canada). To do this, four holes with a depth of 25 mm were drilled at pre-defined positions as depicted in Fig. 3. In order to get a good representation of the temperature distribution within the block, probes were inserted into the block to measure temperature at the geometrical center (center), midway between the geometrical center and the edge (mid), close to the edge (edge) and close to the corner (corner). Tempering was terminated when at least −5 °C was attained at all probe locations.

Surface temperature was measured immediately after tempering using a thermal camera (Model PI200, Optris, Germany). The frozen block was positioned so that the camera was able to see the whole upper surface. The emissivity setting was adjusted to be 0.95, since water and most organic materials such as foods have an emissivity close to 0.95 (Powitz, 2006). A rectangular area that included only the shrimp block was defined on the acquired thermograms. Then; minimum, maximum, and average temperatures within this area were obtained. Standard deviation of the temperatures observed at the upper surface was also calculated to provide a measure of surface temperature distribution.

2.4. Power measurement

During RF tempering, power absorbed by the frozen block of shrimp was estimated using the electrical current (I) values displayed on the PLC screen of the radio frequency oven from the relationship of $P = VI$. To do this, the current readout during system running without load at the adjusted electrode gap was subtracted from the current value displayed during tempering (with load), and the result was multiplied by 3000 V (voltage applied to top electrode as provided by the manufacturer).

An approach similar to the IMPI 2-liter test as detailed by Buffler (1993) was also used to determine the power converted to heat (heat

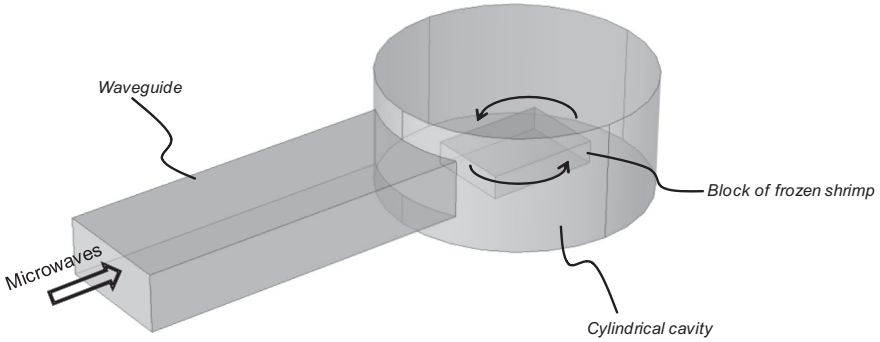

Fig. 1. Schematic of the microwave tempering experimental setup.

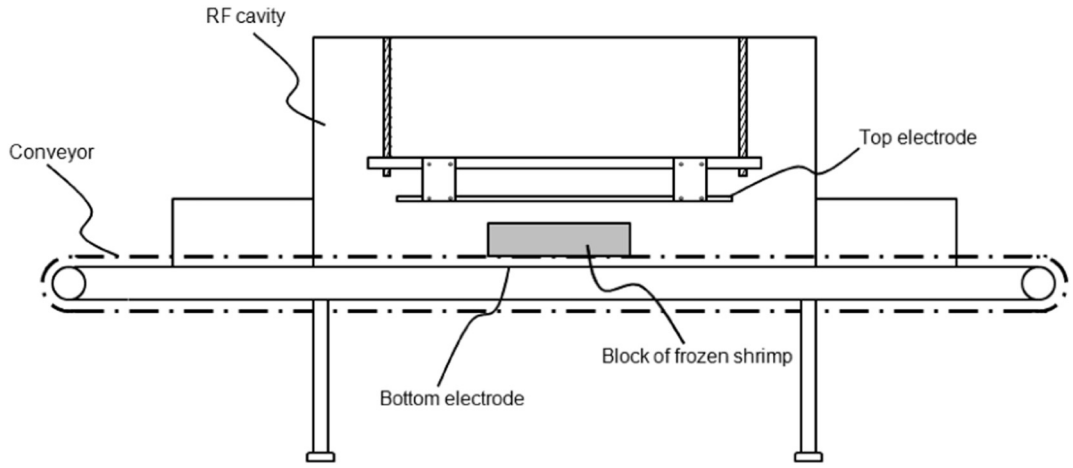

Fig. 2. Schematic of the radio frequency tempering experimental setup.

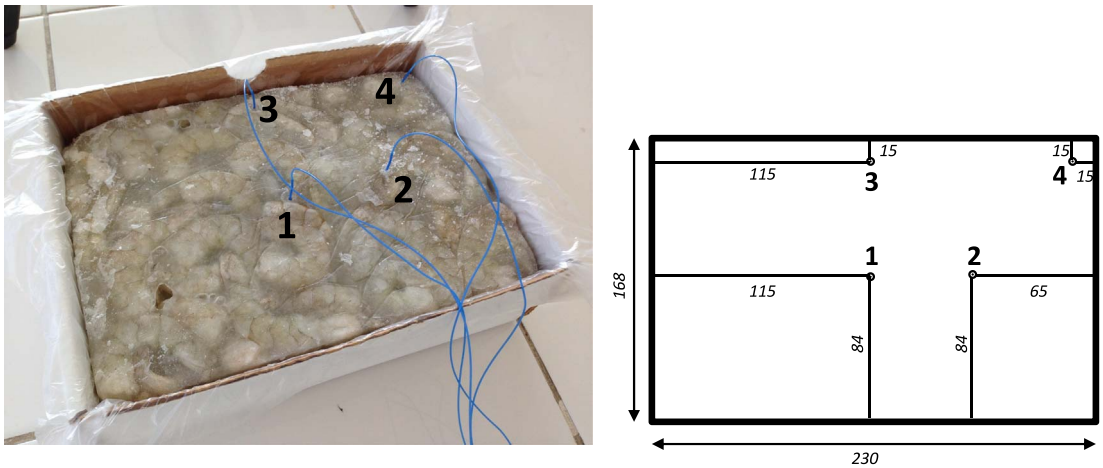

Fig. 3. Locations of fiber optic temperature probes (1: center, 2: mid, 3: edge, 4: corner; all probes were placed 25 mm deep from the top surface; dimensions are in mm).

generation rate) during microwave and RF tempering. It was possible to calculate heat generation rate using this procedure for the beginning of the experiment where no phase change took place. Within this region it is reasonable to assume that heat converted from the absorbed power was only used to raise the temperature of the block and not as latent heat. To use this procedure, an average temperature for the whole block was approximated by averaging the temperature readings taken at four different locations using the fiber optic probes. By doing this, it was assumed that the four probes (center, mid, edge, and corner) were distributed within the block in a way that their average could reasonably represent the volume-average temperature. Heat generation rate for the whole block was calculated in Watts by using Eq. (1).

$$Q = mc_p \frac{dT}{dt} \tag{1}$$

where m is the mass of the frozen block (1.75 kg), c_p is the average of the c_p values at the initial temperature and the temperature at the end of the linear region (usually the first 2 min) of time-average temperature curve, and dT/dt is the heating rate (slope of the linear region). The same procedure was used by Farag et al. (2010) to calculate heat generation rate (power absorption as they defined it) during tempering of beef blends in a 50 Ω RF unit where they assumed no phase change and ignored conductive heat transfer contribution.

2.5. Tempering uniformity

Temperature uniformity index (λ) value, which is simply the ratio of the rise in standard deviation (σ) to the rise in average temperature (μ) over treatment time ($\frac{\Delta\sigma}{\Delta\mu}$), was defined by Wang et al. (2005) and employed by several researchers (Zhou et al., 2015; Zhang et al., 2015; Chen et al., 2015) in order to assess the uniformity of electromagnetic heating. Smaller index values indicate better heating uniformity. This value, however, lacks in providing information on how heating progresses during treatments since it uses only the initial and final values. To better understand the effect of process parameters (microwave power and electrode gap) on heating behavior, heating uniformity index (λ_N) value that takes into account not only the initial and final values of the temperatures, but also all the other values in between was alternatively defined (Eq. (2)). Eq. (2) yields a value similar to relative mean square error (RMSE) which represents a cumulative variation of the observations and is thought to better reflect the uniformity of the tempering treatments. This value was calculated using the internal temperature readings since only the internal temperatures were continuously measured during the experiments.

$$\lambda_N = \sqrt{\frac{1}{N}\sum_{i=1}^{N}\left(\frac{\sigma_i}{\mu_i}\right)^2} \tag{2}$$

2.6. Statistical analysis

Uniformity index values reported are the means of two replicates. Statistical analysis was performed using one-way ANOVA and Tukey's HSD post-hoc test where $p < 0.05$ was considered statistically significant.

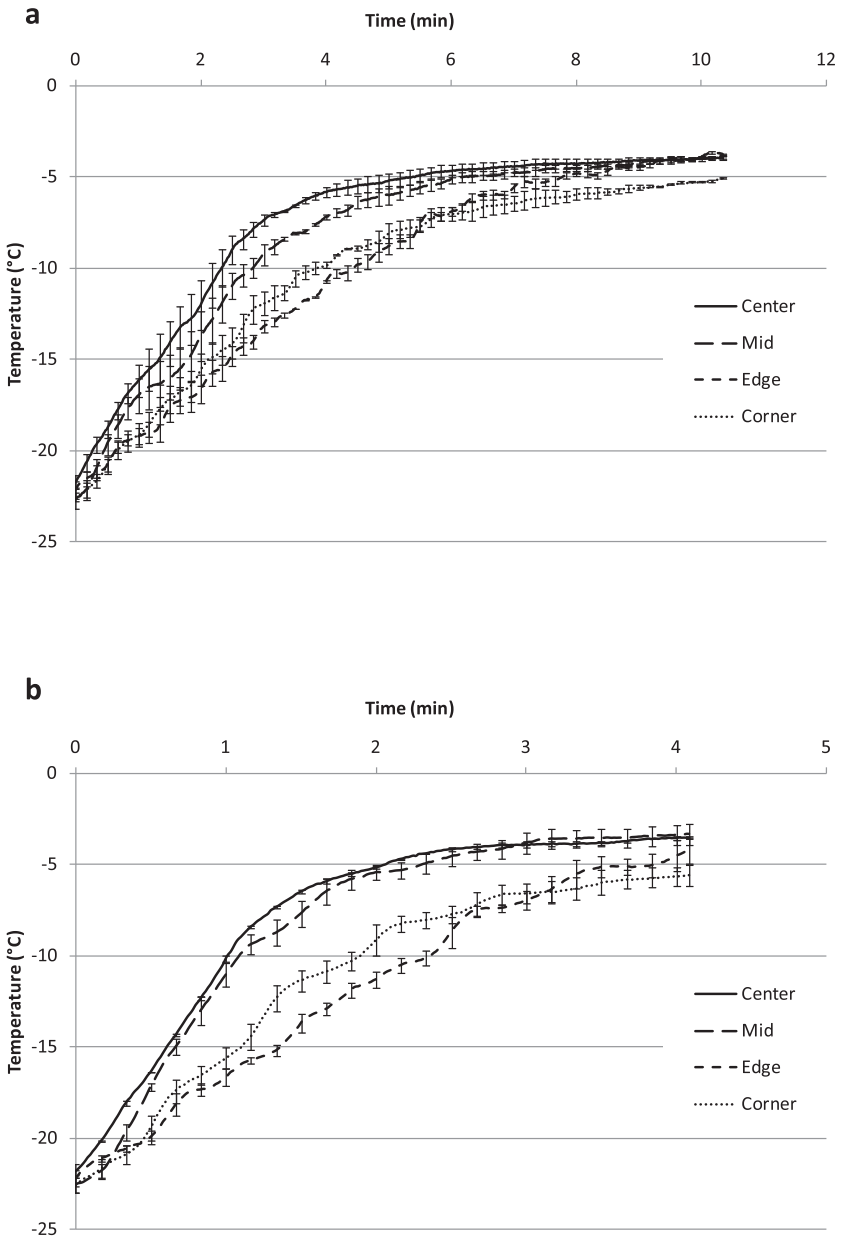

Fig. 4. Internal temperature profiles during microwave tempering at a) 500 W and b) 1 kW.

3. Results and discussion

3.1. Microwave tempering

Time needed for temperature increase from the initial (~−22 °C) to between − 5 and − 3 °C at all four locations where the fiber optics were inserted was about 10 and 4 min at power settings of 500 W and 1 kW, respectively (Fig. 4a and b). Temperature increase at the center was found to be the fastest, since the center of the block was directly facing the waveguide throughout the experiment. Temperature increase at the corner and the edge was the slowest, since these parts of the block were moving in and out of the path of the waveguide. Temperature at the locations also fluctuated more for the same reason. No overheating was observed at any of the four internal probe locations for either power setting.

Thermal images of the upper surface of the block after microwave tempering were presented in Fig. 5 for both power settings (two repetitions were shown for each power setting). Minimum, maximum and average temperatures were also depicted on the images. Although the surface temperature distributions appeared to be similar, local overheating was more pronounced in case of the higher power setting (1 kW). It can be clearly seen from these images that there were completely thawed-out spots on the upper surface where temperatures were as high as 7.3 °C (for 500 W) and 18.6 °C (for 1 kW). Majority of the surface, however, was below freezing.

Although rotating the frozen food helps minimize temperature differences during microwave tempering, surface overheating still remains a problem. Surface layer, when there is free water, absorbs much more energy than do still-frozen inner layers which consequently leads to a decrease in penetration depth and accelerated heating at the surface. Rosenberg and Bögl (1987) reported that the three orders of magnitude difference between the dielectric loss factors of frozen and liquid water can easily cause runaway heating as soon as a part of the product is completely thawed. Brewer (2005) also reported that at temperatures near 0 °C, the outer layer of meat can absorb significant amounts of energy, resulting in overheating near the surface.

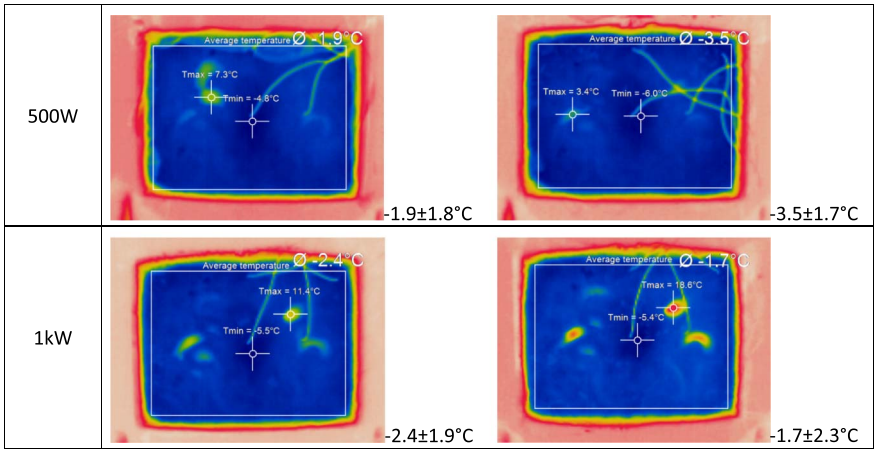

Fig. 5. Thermal images (surface temperature distribution) of shrimp block tempered by microwave.

3.2. Radio frequency tempering

Time needed for temperature increase from the initial to between −5 and −3 °C at all internal locations were about 11 and 7 min at electrode gap settings of 160 and 150 mm, respectively for both without rotation (Fig. 6a and b) and with rotation (Fig. 7a and b). While similar heating rates were observed for the center and mid locations, the corner and edge of the block heated faster than did the center and mid locations for both electrode gap settings and moving conditions. Alfaifi et al. (2016) also observed higher temperatures near the edges and corners when compared to the center during RF heating of raisins packed in a rectangular shape. Overheating of corners and sharp edges during RF heating appears to be a common problem and has been reported also by other researchers (Ikediala et al., 2002; Alfaifi et al., 2014; Zhang et al., 2015; Huang et al., 2015). It has been reported that current density concentrates along the edges of the electrode causing non-uniform thermal effects (Schomaker and Rosenberg, 2016). Alfaifi et al. (2016) reported that this problem can be partially overcome and heating uniformity can be improved by rounding the corners and reducing sharp edges. Bending the electrodes was also studied by Alfaifi et al. (2016) as a potential strategy to improve heating uniformity by altering the electric field inside an RF system.

Uniform distribution of temperatures throughout the upper surface of the RF-tempered block can be clearly seen from the thermal images presented in Fig. 8 (without rotation) and Fig. 9 (with rotation). In contrast to microwave tempering, no overheating was observed on the upper surface upon RF tempering with all the temperatures throughout the surface being < 0 °C (Figs. 8 and 9). The highest temperature at the upper surface resided near the corner of the block as expected.

3.3. Power absorption

Change of absorbed power (calculated from the electrical current readouts during RF tempering) with time of RF tempering without rotation was presented in Fig. 10 for both electrode gap settings. The absorbed power profile during RF tempering with rotation (data not presented) was almost identical. According to Fig. 10, power absorption was found to linearly increase from an initial value of 428 ± 6 W to a peak value of 612 ± 0 W for the gap setting of 150 mm within the first 2 min of tempering, and from an initial value of 258 ± 17 W to a peak value of 381 ± 4 W for the gap setting of 160 mm within the first 3 min of tempering. Then, both absorbed power values continuously decreased until the end of the treatment. This behavior of power absorption may be attributed to the variation in electrical conductivity during phase transition from ice to water, and can be explained by the effect on electrical conductivity of the concentration and mobility of ions which carry charges along the electric field (Zhang, 2009). During freezing, ions are excluded from the ice leading to increased ion concentration in the remaining solution (Pham, 2008). It is known that even at −25 °C, there is still about 5% water in unfrozen state (Hall, 1997). Although greater concentration of ions favors ionic conduction, electrical conductivity drops since ion mobility is hindered by the high viscosity of the liquid phase at low temperatures (Buera et al., 2011). In addition, too high an ionic concentration has been reported to possibly decrease electrical conductivity due to increased ionic interaction (Reddy et al., 2002). As ice turns into liquid water during tempering, electrical conductivity increases due to increased mobility of the dissolved ions. This in turn leads to an increase in current. However, as more water turns into unfrozen state, the solution becomes less concentrated with ions which leads to a drop in electrical conductivity. These phenomena are thought to be responsible for the variation in current during the phase change process and characteristic to radio frequency tempering.

The values of heat generation rate (calculated from the heating rates) were found to be 355 ± 28 W for 150 mm gap setting and 240 ± 7 W for 160 mm gap setting. These values were constant for the first 2 min of tempering where a linear increase in temperature, hence a constant rate of heating was observed. Although the power absorption and the heat generation rate were comparable initially, they differed markedly as tempering progressed. The power absorption kept increasing, whereas the heat generation rate remained constant during the first 2 min. This suggested that parts of the block may have experienced a larger temperature rise resulting in an increase in the dielectric constant (responsible for absorbed power) which apparently was not reflected in the measured temperatures that were used for calculating the heat generation rate. The increase in specific heat within the temperature range studied may also have caused this observation by offsetting the effect of increasing dielectric constant. Farag et al. (2010) reported increasing heat generation rate with tempering time for RF tempering of 50:50 blend of lean beef and fat, although the rate of heating linearly decreased throughout their experiment. They attributed this observation to the increase in specific heat as the temperature rose from −18 to −5 °C.

Heat generation rates during MW tempering at 500 W and 1 kW were found to be 340 ± 26 W and 809 ± 36 W, respectively. Although the heat generation rates during MW tempering at 500 W and RF tempering at a gap setting of 150 mm were similar, RF tempering was completed in a shorter period of time presumably due to the greater increase in dielectric loss factor with temperature at lower frequencies within the temperature range studied. Basaran-Akgul et al. (2008) reported that at −5 °C, dielectric loss factor of frozen beef at 27 MHz was about 10 times greater than that at 915 MHz. Farag et al. (2008b) also reported that dielectric properties (particularly dielectric loss factor) of lean beef-fat blends at 27.12 MHz were significantly

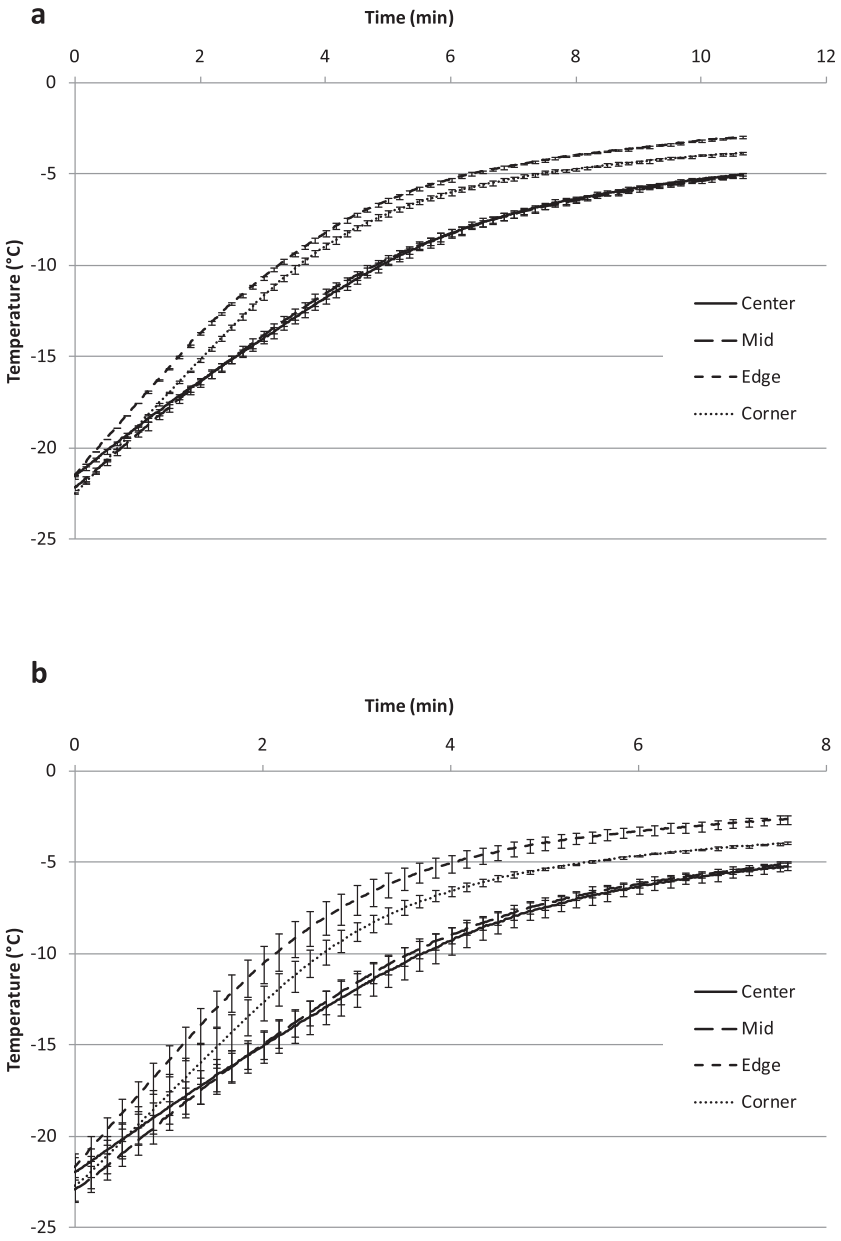

Fig. 6. Internal temperature profiles during radio frequency tempering without rotation a) gap setting 160 mm b) gap setting 150 mm.

higher than those at 896 MHz at most temperatures.

3.4. Tempering uniformity

Temperature uniformity index (λ) values calculated from internal and surface temperature measurements were presented in Table 1. From the table, microwave thawing at 500 W was the most uniform treatment in terms of internal temperature distribution while all other treatments were comparable. No significant difference was found between the surface temperature uniformity index values, although local surface overheating appeared to be a problem of microwave tempering. Electrode gap setting in the studied range did not influence heating uniformity. Li et al. (2016) also observed no significant effect on heating uniformity during RF heating of chili powder within an electrode gap range of 95–135 mm.

From the heating uniformity index (λ_N) values presented in Table 2, it can be seen that tempering was the least uniform for microwave treatment at 1 kW. According to Table 2, RF heating was more uniform at 160 mm in comparison to 150 mm when no rotation was employed. Rotating the block during RF tempering appeared to improve heating uniformity when the electrode gap setting was 150 mm. This observation may be attributed to the variation of voltage over the surface of the top electrode which was reported to increase from its minimum value at the feed point to a maximum value at the electrode edge (Wang et al., 2010). Wang et al. (2015) reported a maximum of 7% (with load) and 12% (without load) variation in voltage for a 400 × 830 mm electrode. A better uniformity of heating was also achieved by Wang et al. (2010) by moving the sample back-and-forth along the length of the electrode. Wang et al. (2014), however, reported no noticeable improvement in heating uniformity due to movement of the conveyor during hot air assisted RF drying of macadamia nuts.

In the present study, rotation had no effect on heating uniformity when the gap setting was 160 mm. It is thought that RF power within the block was already uniform at this gap setting, hence no further improvement in heating uniformity was observed. Earlier research (Huang et al., 2015; Tiwari et al., 2011; Birla et al., 2008) have shown that RF heating uniformity increases when the product is vertically moved toward the center of the electrodes (which was the case for

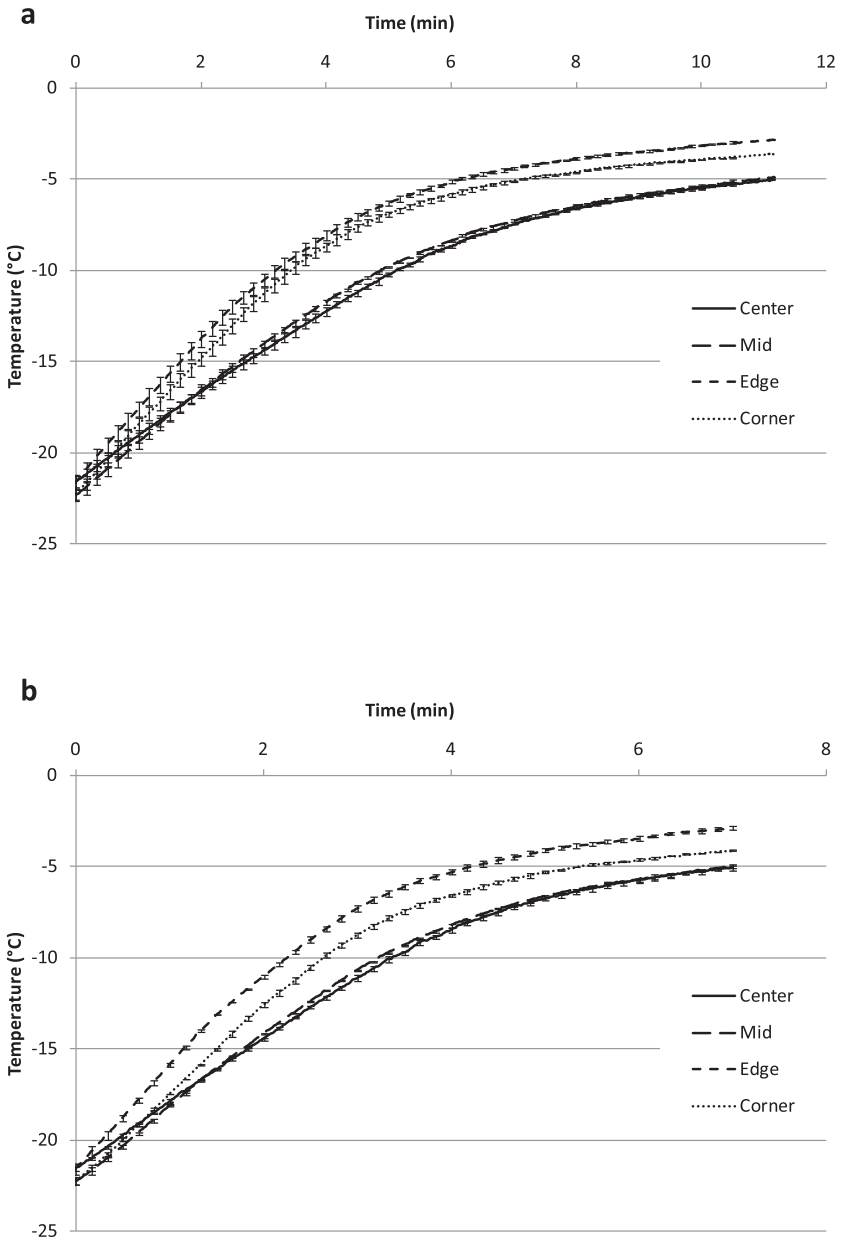

Fig. 7. Internal temperature profiles during radio frequency tempering with rotation a) gap setting 160 mm b) gap setting 150 mm.

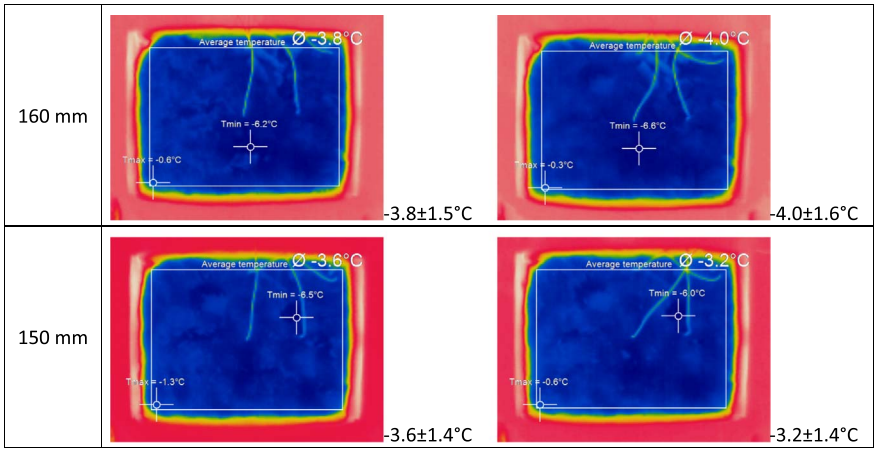

Fig. 8. Thermal images (surface temperature distribution) of shrimp block tempered by radio frequency without rotation.

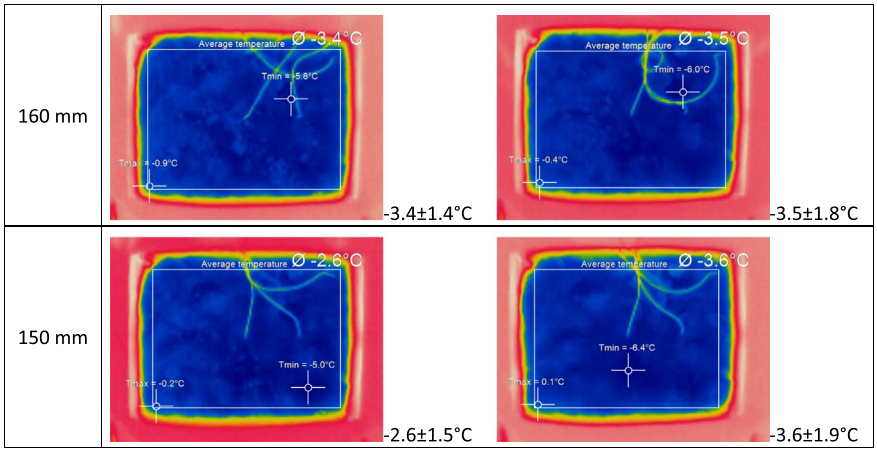

Fig. 9. Thermal images (surface temperature distribution) of shrimp block tempered by radio frequency with rotation.

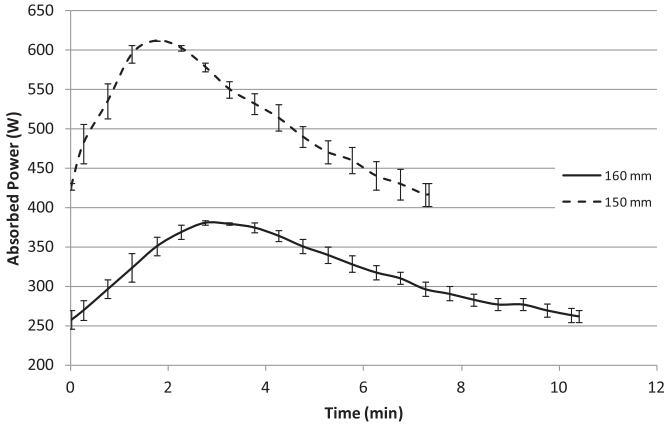

Fig. 10. Change of absorbed power with time during radio frequency tempering.

Table 1
Internal and surface temperature uniformity index (λ) values calculated from the initial and final temperature readings.

Tempering method			$\lambda_{internal}$	$\lambda_{surface}$
Microwave	500 W		0.0093 ± 0.0080[a]	0.0678 ± 0.0083[a]
	1 kW		0.0395 ± 0.0074[b]	0.0865 ± 0.0066[a]
RF	150 mm	Without rotation	0.0339 ± 0.0079[b]	0.0433 ± 0.0036[a]
		With rotation	0.0369 ± 0.0010[b]	0.0706 ± 0.0222[a]
	160 mm	Without rotation	0.0298 ± 0.0041[ab]	0.0592 ± 0.0058[a]
		With rotation	0.0388 ± 0.0044[b]	0.0659 ± 0.0158[a]

Table 2
Heating uniformity index (λ_N) values calculated from the internal temperature profiles.

Tempering method			λ_N
Microwave	500 W		0.1884 ± 0.0080[a]
	1 kW		0.2890 ± 0.0082[b]
RF	150 mm	Without rotation	0.2313 ± 0.0004[c]
		With rotation	0.1803 ± 0.0181[a]
	160 mm	Without rotation	0.1861 ± 0.0039[a]
		With rotation	0.2127 ± 0.0141[ac]

160 mm gap setting). This way the problem of electrical field concentration at the surfaces resulting from the product being closer to one of the electrodes is minimized.

4. Conclusion

Microwave and radio frequency tempering were compared experimentally in this study. For the comparison to be meaningful, microwave tempering was conducted at 915 MHz, the frequency which most industrial scale microwave equipment operate at due to the ability of microwaves at this frequency to penetrate large samples (Decareau and Peterson, 1986; Hassan et al., 2015). Radio frequency used in the study (27.12 MHz) is even more suitable for treating large samples due to its much larger penetration depth.

Tempering of the shrimp block by both methods was achieved within comparable periods of time. Central parts of the frozen block heated more rapidly during microwave tempering, whereas the corners and edges heated more rapidly during RF tempering. Internal temperature distribution upon tempering treatments was found to be quite uniform, whereas local surface overheating appeared to be a problem of microwave treatment as revealed by the thermograms acquired by infrared imaging. Although tempering rather than full thawing can be an effective strategy to avoid the problem of runaway heating associated with microwave application, it was shown in this study that microwave tempering can easily lead to runaway heating if not carefully controlled. Radio frequency, however, allows to achieve temperatures close to 0 °C without jeopardizing the product's quality.

Practical application

Project findings will be helpful for processors who consider rapid heating technologies for tempering purposes.

Acknowledgment

The authors are grateful to the Scientific and Technical Research Council of Turkey, TUBITAK (Project no. 109O772) and Mersin University (Project no. BAP-FBE GMB (ST) 2012-2 DR) for funding the equipment used in this study.

References

Alfaifi, B., Tang, J., Jiao, Y., Wang, S., Rasco, B., Jiao, S., & Sablani, S. (2014). Radio frequency disinfestation treatments for dried fruit: Model development and validation. *Journal of Food Engineering, 120*, 268–276.

Alfaifi, B., Tang, J., Rasco, B., Wang, S., & Sablani, S. (2016). Computer simulation analyses to improve radio frequency (RF) heating uniformity in dried fruits for insect control. *Innovative Food Science & Emerging Technologies, 37*, 125–137.

Basaran-Akgul, N., Basaran, P., & Rasco, B. (2008). Effect of temperature (− 5 to 130 °C) and fiber direction on the dielectric properties of beef *Semitendinosus* at radio frequency and microwave frequencies. *Journal of Food Science*, *73*(6), E243–E249.

Birla, S., Wang, S., & Tang, J. (2008). Computer simulation of radio frequency heating of model fruit immersed in water. *Journal of Food Engineering*, *84*(2), 270–280.

Brewer, M. (2005). Microwave processing, nutritional and sensory quality. In H. Schubert, & M. Regier (Eds.), *The microwave processing of foods*. Boca Raton, FL, USA: CRC Press.

Buera, M. P., Roos, Y., Levine, H., Slade, L., Corti, H. R., Reid, D. S., ... Angell, C. A. (2011). State diagrams for improving processing and storage of foodsi biological materials, and pharmaceuticals (IUPAC technical report). *Pure and Applied Chemistry*, *83*(8), 1567–1617.

Buffler, C. R. (1993). *Microwave cooking and processing: engineering fundamentals for the food scientist, AVI*. New York: van Nostrand Reinhold.

Chen, L., Wang, K., Li, W., & Wang, S. (2015). A strategy to simulate radio frequency heating under mixing conditions. *Computers and Electronics in Agriculture*, *118*, 100–110.

Choi, E. J., Park, H. W., Chung, Y. B., Park, S. H., Kim, J. S., & Chun, H. H. (2017). Effect of tempering methods on quality changes of pork loin frozen by cryogenic immersion. *Meat Science*, *124*, 69–76.

Decareau, R. V., & Peterson, R. A. (1986). Microwave technology. *Microwave processing and engineering*. Chichester, UK: Ellis Horwood.

Dubey, M. K., Janowiak, J., Mack, R., Elder, P., & Hoover, K. (2016). Comparative study of radio-frequency and microwave heating for phytosanitary treatment of wood. *European Journal of Wood and Wood Products*, *74*(4), 491–500.

Farag, K., Lyng, J. G., Morgan, D. J., & Cronin, D. A. (2008a). A comparison of conventional and radio frequency tempering of beef meats: Effects on product temperature distribution. *Meat Science*, *80*, 488–495.

Farag, K., Lyng, J. G., Morgan, D. J., & Cronin, D. A. (2008b). Dielectric and thermophysical properties of different beef meat blends over a temperature range of − 18 to + 10 °C. *Meat Science*, *79*, 740–747.

Farag, K., Lyng, J. G., Morgan, D. J., & Cronin, D. A. (2011). A comparison of conventional and radio frequency thawing of beef meats: Effects on product temperature distribution. *Food and Bioprocess Technology*, *4*(7), 1128–1136.

Farag, K., Marra, F., Lyng, J. G., Morgan, D. J., & Cronin, D. A. (2010). Temperature changes and power consumption during radio frequency tempering of beef lean/fat formulations. *Food and Bioprocess Technology*, *3*(5), 732–740.

Fu, Y.-C. (2004). Fundamentals and industrial applications of microwave and radio frequency in food processing. In J. S. Smith, & Y. H. Hui (Eds.), *Food processing: Principles and applications*. Oxford, UK: Blackwell Publishing.

Hall, G. M. (1997). *Fish processing technology* (2nd ed.). London, UK: Blackie Academic & Professional.

Hassan, H. F., Tola, Y., & Ramaswamy, H. S. (2015). Radio-frequency and microwave applications: Similarities, advantages, and limitations. In G. B. Awuah, H. S. Ramaswamy, & J. Tang (Eds.), *Radio-frequency heating in food processing: Principles and applications*. Boca Raton, FL, USA: CRC Press.

Huang, Z., Zhu, H., Yan, R., & Wang, S. (2015). Simulation and prediction of radio frequency heating in dry soybeans. *Biosystems Engineering*, *129*, 34–47.

Ikediala, J. N., Tang, J., Hansen, J., Drake, S. R., & Wang, S. (2002). Quarantine treatment of fruits using radio frequency energy and an ionic-water-immersion technique. *Postharvest Biology and Technology*, *24*, 25–37.

Li, B., & Sun, D. W. (2002). Novel methods for rapid freezing and thawing of foods - A review. *Journal of Food Engineering*, *54*, 175–182.

Li, Y., Zhang, Y., Lei, Y., Fu, H., Chen, X., & Wang, Y. (2016). Pilot-scale radio frequency pasteurization of chili powder: Heating uniformity and heating model. *Journal of the Science of Food and Agriculture*, *96*, 3853–3859.

Pham, Q. T. (2008). Advances in food freezing/thawing/freeze concentration modelling and techniques. *Japan Journal of Food Engineering*, *9*(1), 21–32.

Powitz, R. W. (2006). Infrared thermometry. *Food safety magazine, October/November 2006*. Retrieved from www.foodsafetymagazine.com/magazine-archive1/octobernovember-2006/infrared-thermometry/ Accessed on 08 October 2016 .

Reddy, K. R., Saichek, R. E., Sara, M. N., & Everett, L. G. (2002). Electrokinetic removal of phenanthrene from kaolin using different surfactants and cosolvents. *Evaluation and remediation of low permeability and dual porosity environments*. Saline, MI, USA: ASTM International.

Rosenberg, U., & Bögl, W. (1987). Microwave thawing, drying and baking in the food industry. *Food Technology*, *41*, 85–91.

Schomaker, K. T., & Rosenberg, A. (2016). Reduction of RF electrode edge effect. *US Patent no. 9381057 B2*.

Tiwari, G., Wang, S., Tang, J., & Birla, S. L. (2011). Analysis of radio frequency (RF) power distribution in dry food materials. *Journal of Food Engineering*, *104*(4), 548–556.

Wang, D. I. C., & Goldblith, S. A. (1976). *Dielectric properties of foods*. MA, USA: U.S. Army Natick Research and Development Command.

Wang, K., Chen, L., Li, W., & Wang, S. (2015). Evaluating the top electrode voltage distribution uniformity in radio frequency systems. *Journal of Electromagnetic Waves and Applications*, *29*(6), 763–773.

Wang, S., Tiwari, G., Jiao, S., Johnson, J. A., & Tang, J. (2010). Developing postharvest disinfestations treatments for legumes using radio frequency energy. *Biosystems Engineering*, *105*(3), 341–349.

Wang, S., Yue, J., Tang, J., & Chen, B. (2005). Mathematical modelling of heating uniformity for in-shell walnuts subjected to radio frequency treatments with intermittent stirrings. *Postharvest Biology and Technology*, *35*, 97–107.

Wang, Y., Zhang, L., Gao, M., Tang, J., & Wang, S. (2014). Pilot-scale radio frequency drying of macadamia nuts: Heating and drying uniformity. *Drying Technology*, *32*, 1052–1059.

Yarmand, M., & Homayouni A. R. (2011). Microwave processing of meat, Microwave heating, Dr. Usha Chandra (Ed.), ISBN: 978-953-307-573-0, InTech, Retrieved from: www.intechopen.com/books/microwave-heating/microwave-processing-of-meat, Accessed on 07 October 2016.

Zhang, H. (2009). Electrical properties of foods. In G. B. Canovas (Vol. Ed.), *Food engineering. vol. 1*. Oxford, UK: Eolss Publishers Co. Ltd.

Zhang, P., Zhu, H., & Wang, S. (2015). Experimental evaluations of radio frequency heating in low-moisture agricultural products. *Emirates Journal of Food and Agriculture*, *27*, 662–668.

Zhao, Y., Flugstad, B., Kolbe, E., Park, J. W., & Wells, J. H. (2000). Using capacitive (radio frequency) dielectric heating in food processing and preservation - A review. *Journal of Food Process Engineering*, *23*, 25–55.

Zhou, L., Ling, B., Zheng, A., Zhang, B., & Wang, S. (2015). Developing radio frequency technology for postharvest insect control in milled rice. *Journal of Stored Products Research*, *62*, 22–31.